JOURNAL OF MATERIALS SCIENCE: MATERIALS IN ELECTRONICS 2 (1991) 40–45

Some physical properties of fluorine-doped SnO_2 films prepared by spray pyrolysis

H.H. AFIFY*
Department of Physics, National Research Centre, Dokki, Cairo, Egypt

R. S. MOMTAZ
Department of Physics and Mathematics, Faculty of Engineering, Suez Canal University, Port-Said

W. A. BADAWY[†], S. A. NASSER[§]
Departments of [‡]Chemistry and [§]Physics, Faculty of Science, Beni-Suef, Cairo University, Egypt

Thin films of undoped and fluorine-doped tin oxide have been prepared on fused silica substrates by a spray pyrolysis technique. Structural, optical and electrical properties were studied. Fluorine doping increased the degree of crystallinity and preferred orientation as well as the figure of merit (23.9×10^{-3} at 0.5 μm). The refractive index, n, showed a considerable decrease (2.2–1.85) on fluorine doping. The direct allowed transition for fluorine-doped tin oxide was 0.1 eV higher than that of undoped material.

1. Introduction

The high transparency of tin oxide semiconductors, combined with their mechanical hardness adherence and good environmental stability, has opened up numerous applications for them, including electrodes for optoelectronic devices, photovoltaics, photoelectrochemical cells, electroluminescent cells and solar collectors [1, 2].

There are many techniques including sputtering, evaporation and chemical vapour or spray deposition, by which these materials may be deposited. The spray deposition method is particularly attractive because of its simplicity. It is fast, inexpensive and vacuumless, and is suitable for mass production. Moreover, this technique would make it possible for the developing countries to apply this technique by their own means.

It is well known that the conductivity of tin oxide films can be enhanced by appropriate doping [3, 4]. It was observed that F-doped tin oxide films have a higher conductivity, transmissivity and infrared reflection than the undoped films [5]. The cause of this enhancement has not been explained fully. Recently, some reports have suggested that the structure plays a major role in this behaviour [6]. In view of this, undoped and fluorine-doped tin oxide thin films have been prepared using the spray pyrolysis technique. The relationships between the structure, optical and electrical properties of the films were investigated.

2. Experimental procedure

The spray pyrolysis technique used is basically a chemical deposition technique in which fine droplets of the desired material solution are sprayed onto a heated substrate. A continuous film is formed on the hot substrate by thermal decomposition of the material droplets. The spray equipment [7] and furnace are shown in Fig. 1. The atomizer, which is the main part, consists of a nozzle mounted in a 100 ml glass round-bottom flask. Filtered compressed air is used as the carrier gas and the flow is controlled by a flow meter. The furnace is an electrically heated stainless steel cylinder, 10 cm long and 5 cm diameter, with an aperture 0.1 cm below the upper surface for inserting the thermocouple. The furnace temperature is adjusted to $\pm 2\,^{\circ}C$ by using a variac transformer. Using this arrangement an aerosol with very small droplet size reaches the heated substrate.

Tin oxide films are formed by spraying a solution of 0.6 M $SnCl_4$ in ethyl alcohol on cleaned hot-fused silica glass substrates. Fluorine-doped tin oxide films are prepared by spraying an equimolar (0.6 M) solution of $SnCl_4$ and NH_4F. The deposition parameters are: air flow rate $5\,l\,min^{-1}$, substrate temperature $450 \pm 2\,^{\circ}C$, deposition time 1–12 min.

Structural analysis was carried out using Phillips X-ray diffraction equipment model PW/1710 with an Ni filter and CuK_α radiation ($\lambda = 0.1542$ nm) at 40 kV and 30 mA. For peak profile analysis the speeds of the X-ray diffractometer are chosen to give a good resolution of 4 cm/degree of Bragg angle.

The optical measurements were made using the recording double-beam lambda 4B Perkin–Elmer spectrophotometer. The sheet resistance was measured using the four-probe method, and all measurements were carried out at room temperature.

*Author to whom correspondence should be addressed.

0022–2461/91 $03.00 + .12

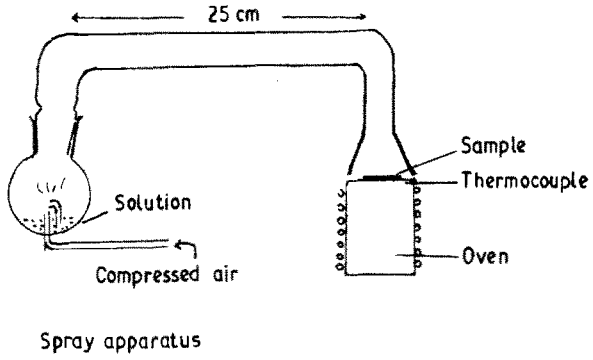

Figure 1 Schematic diagram of the spray pyrolysis system.

3. Results and discussion

3.1. Structural studies

X-ray diffraction patterns of the deposited films of undoped and F-doped SnO_2 with different film thickness are shown in Fig. 2. The d-spacings calculated from 2θ and the relative intensities (I/I_0) for the various planes are estimated from the recorded counting rate. The values of d agree with ASTM data for SnO_2 powder [8]. General examination of all the patterns revealed that addition of fluorine at a concentration of 10% produced no additional lines representing either dopant or any other unwanted phase. These data are similar to those obtained by Sundaram and Bhagavat [9]. However, the relative diffraction intensity (I/I_0) for each lattice plane did not agree well with the ASTM data. Agashe *et al.* [10] reported a similar observation in the case of undoped SnO_2 films. This is probably a result of the different effective thickness of thin films and powder samples.

Lattice constants a and c of the thin films were determined using high-angle reflections [11]. The values obtained in the present study were compared with existing data as given in Table I. The values of a, c, and the volume of the unit cell, v, of the undoped SnO_2 films agree with those obtained from the ASTM card for polycrystalline SnO_2 powder of tetragonal cassiterite structure [8]. The intensity of the diffraction planes of the tin oxide films shows a definite increase on doping with fluorine, as shown in Fig. 2. In addition, some of the planes of F-doped films orient themselves to give maximum reflection, and hence maximum intensity is observed. Thus the crystallinity of undoped SnO_2 thin films is generally poor and a good improvement in the crystallinity is observed for F-doped thin oxide film of thickness, $t = 350$ nm.

Carroland and Slack [12] stated that doping and the thickness of the thin film affect the preferred orientation of the microcrystallites in polycrystalline thin films. An examination was carried out of the preferred orientation planes in the investigated films by studying the peak profiles of planes (1 1 0), (2 0 0) and (3 0 1) because these planes are more sensitive to microcrystallite orientation in SnO_2 [13, 14]. It was observed after analysis of the peak profiles of these planes that the changes in the diffraction peak intensities of (1 1 0) and (3 0 1) planes are less sensitive than in the (2 0 0) plane for describing the preferred orientation of the prepared thin films. Agashe *et al.*

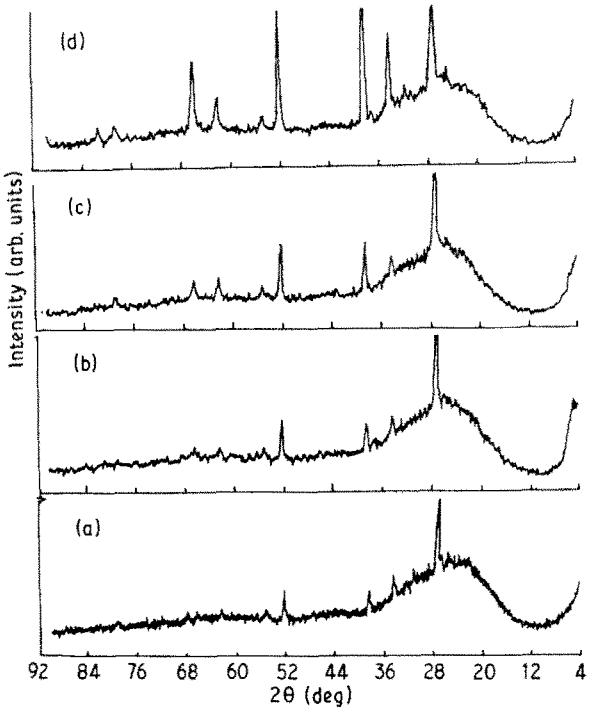

Figure 2 X-ray diffraction patterns of undoped and 10% F-doped SnO_2 films with different thicknesses, t; (a) undoped SnO_2 film, $t = 85$ nm; (b–d) doped SnO_2 films, with $t =$ (b) 85 nm, (c) 172 nm and (d) 350 nm.

[10] reported that thin films of SnO_2 were preferentially oriented along the (2 0 0) plane for higher substrate temperatures ($> 375\,^{\circ}C$). The peak profile intensity of the (2 0 0) plane of undoped SnO_2 films and F-doped films were recorded with good resolution and are shown in Fig. 3. It can be seen from this figure that the intensity of the (2 0 0) diffraction plane increased rapidly on doping with fluorine and on increasing the film thickness. This increase is associated with increasing extent of preferred orientation of the microcrystallites along the (2 0 0) plane. This may be due to an increase in the crystallite size along the (2 0 0) plane. To check this hypothesis, calculation of the cystallite size of the prepared films was carried out from X-ray diffraction patterns using the Scherrer formula [15]. Assuming a homogeneous strain across the crystallites, the average crystallite size, D, for crystallites perpendicular to the (2 0 0) plane was calculated from the relation

$$D = 0.94\lambda/\Delta(2\theta)\cos\theta \qquad (1)$$

where $\Delta(2\theta)$ is the half-peak width of the (2 0 0) diffraction line in radius, θ is the diffraction angle for (2 0 0) and λ is the wavelength of X-rays. This relation is frequently employed to estimate the crystallite size of thin films [16, 17]. The values of the crystallite size obtained are listed in Table I. The crystallite size is seen to between 17 and 30 nm with increasing film thickness of F-doped SnO_2 films. This corresponds to an increase of about 77% in crystallite size which is attributed to the better crystallization conditions originating from the presence of the fluorine dopant. Recently, Agashe *et al.* [10] reported an increase of about 27% in the crystallite size (estimated from X-ray diffraction data) for fluorine-doped SnO_2 films.

TABLE I

No.	Material	Lattice constant, a (nm)	Lattice constant, c (nm)	Unit cell volume, V (nm^2)	Crystallite size, D (nm)	Film thickness (nm)
1	Spec. pure SnO_2 Powder (ASTM data)	0.4738	0.3188	–	–	–
2	Undoped SnO_2 film	0.4715	0.3154	0.701 17	17	85
3	SnO_2: 10% F film	0.4708	0.3151	0.698 43	21	85
4	SnO_2: 10% F film	0.4710	0.3163	0.701 68	24	172
5	SnO_2: 10% F film	0.4731	0.3161	0.707 51	30	350

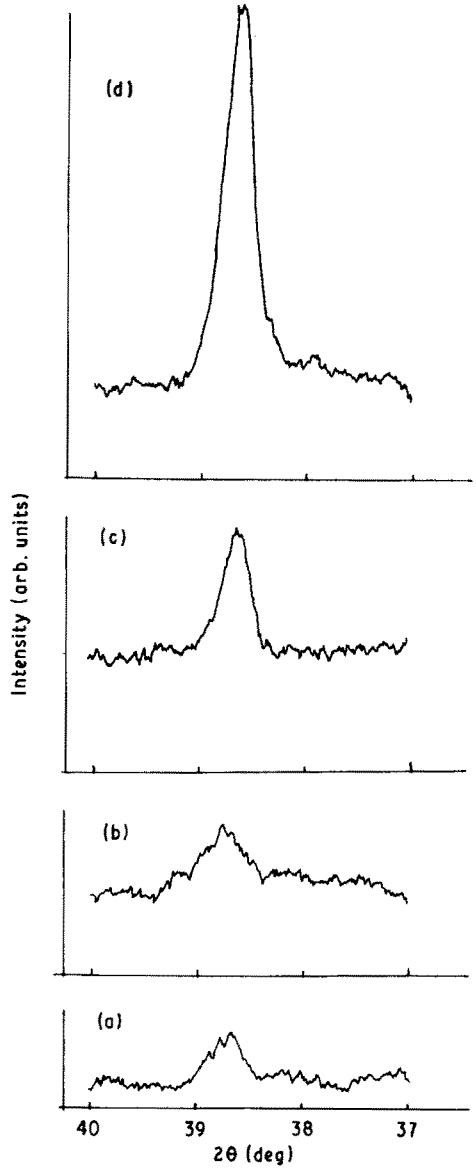

Figure 3 Effect of 10% F doping on the crystallinity of SnO_2 films; (a) undoped SnO_2, t = 85 nm; (b–d) doped SnO_2 with t = (b) 85 nm, (c) 172 nm and (d) 350 nm.

3.2. Optical and electrical properties

The films deposited on fused silica substrates are examined by transmission spectrophotometry in the range 200–900 nm. Fig. 4 illustrates the transmittance spectra (T–λ) for the investigated samples of undoped and F-doped films. A general feature of the T–λ curves is the increasing number of interference extrema with increasing film thickness and doping.

The optical parameter refractive index, n, and thickness of the thin film, t, were calculated from the interference extrema of the T–λ transmittance spectra. The method [18, 19] is based on analysis of the transmittance spectrum of a weakly absorbing film, non-absorbing substrate system. Inverse transmittance can be decomposed into two components

$$\frac{1}{T(\lambda)} = u(\lambda) + c(\lambda)v(\lambda) \tag{2}$$

where $u(\lambda)$ and $v(\lambda)$ consist of exponential and sinusoidal terms, respectively. $u(\lambda)$ and $c(\lambda)$ can be calculated as follows

$$u(\lambda) = \frac{T^+(\lambda) + T^-(\lambda)}{2T^+(\lambda)T^-(\lambda)} \tag{3}$$

$$c(\lambda) = \frac{T^+(\lambda) - T^-(\lambda)}{2T^+(\lambda)T^-(\lambda)} \tag{4}$$

where T^+ and T^- are the experimentally traced envelope curves of the transmission spectrum (see Fig. 4) and λ is the wavelength of the light. Optical parameters n, t and k of a weakly absorbing film are given by

$$n(\lambda) = \tfrac{1}{2}\{[8n_s c(\lambda) + (n_s + 1)^2]^{1/2} + [8n_s c(\lambda) + (n_s - 1)^2]^{1/2}\} \tag{5}$$

$$t = \left\{4\left[\frac{n(\lambda_i)}{\lambda_i} - \frac{n(\lambda_{i+1})}{\lambda_{i+1}}\right]\right\}^{-1} \tag{6}$$

$$k(\lambda) = \frac{\lambda}{4\pi t}\ln\frac{u + (u^2 - c^2 + \sigma)^{1/2}}{2a_+} \tag{7}$$

where

$$\sigma = \left(\frac{n_s^2 - 1}{8n_s}\right)^2\left(n - \frac{1}{n}\right)^2 \tag{8}$$

$$a_+ = \frac{(n+1)^3(n + n_s^2)}{16n_s n^2} \tag{9}$$

For the first order approximation n_s is the index of refraction of the substrate and λ_i, λ_{i+1} are the wavelengths corresponding to two adjacent extrema.

For higher-order approximation

$$n^k(\lambda) = n(\lambda) - vk^2(\lambda) \qquad v = f(n, n_s) \tag{10}$$

The corrections to the refractive index and the film thickness, however, are only necessary for highly absorbing films. For example, if n = 2.5 and k = 0.1, the correction to n is only − 0.001.

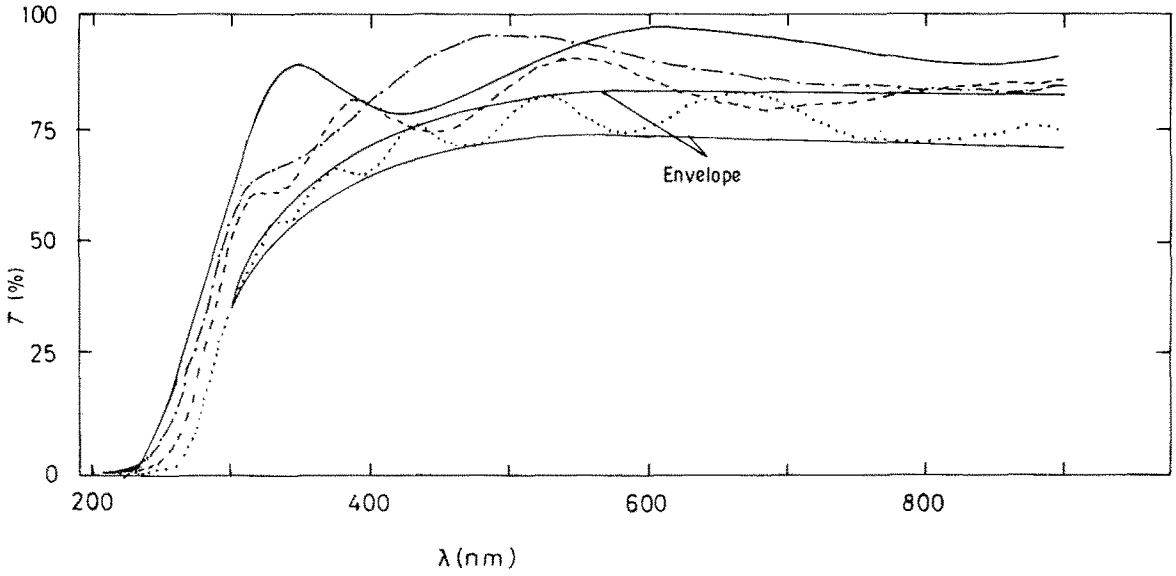

Figure 4 Transmittance, T (%), of undoped SnO_2 and 10% F-doped SnO_2 thin films of different thicknesses as a function of wavelength, λ, from 200–900 nm. (–·–·–) Undoped SnO_2 thin film, t = 85 nm; and doped SnO_2: F with thickness t = (——) 85 nm. (– – –) 172 nm and (· · ·) 350 nm.

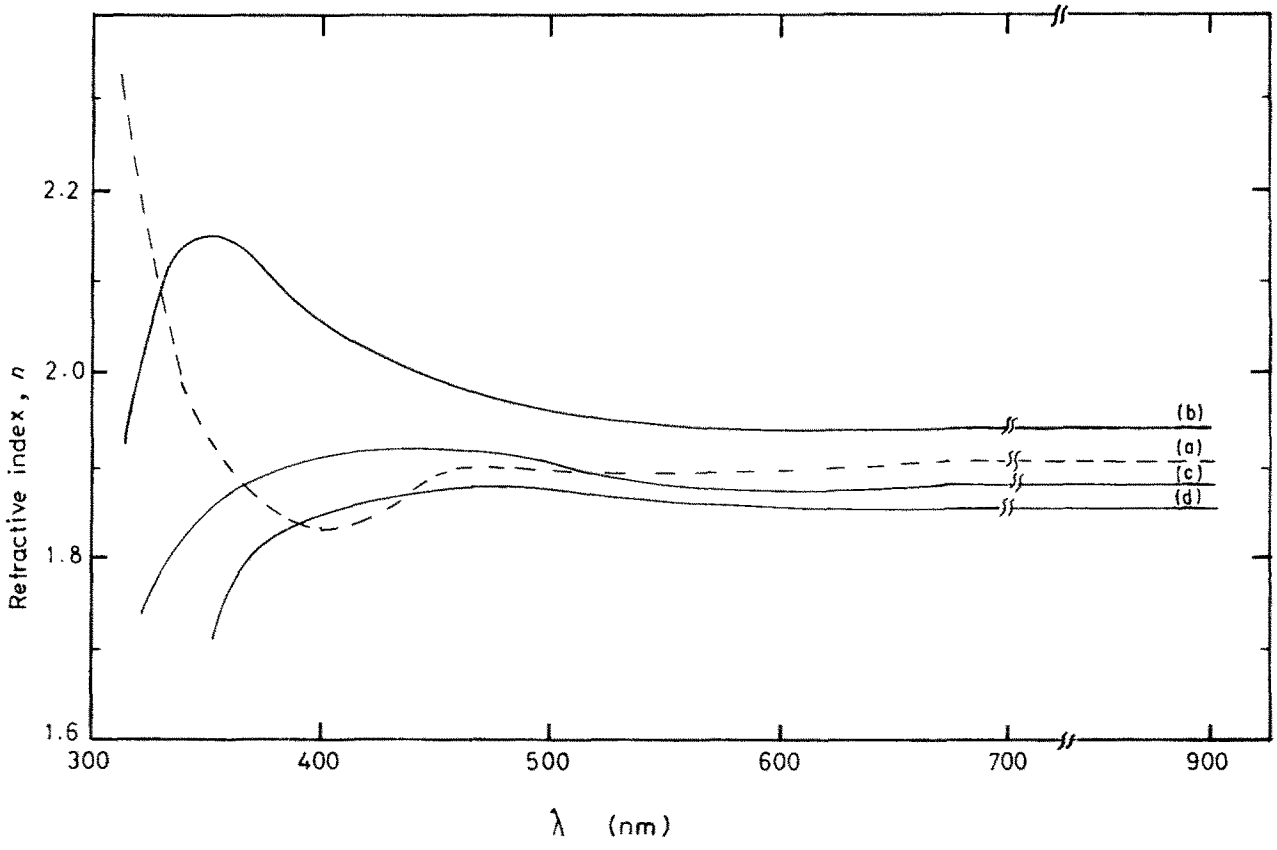

Figure 5 Refractive index, n, as a function of wavelength, λ, from 200–900 nm, (a) for undoped SnO_2 film, t = 85 nm, (b–d) doped SnO_2: F films with t = (b) 85 nm, (c) 172 nm and (d) 350 nm.

By applying this method of calculation on the T–λ curves (Fig. 4), the optical parameter, n, of each film may be calculated. Fig. 5 shows n–λ curves of undoped and F-doped SnO_2 films. The film thickness is also indicated on the figure. The main feature of these plots for undoped and F-doped films is the existence of two regions. First, a non-dispersive region (nearly steady) at λ > 520 nm for the doped and undoped SnO_2 films (t = 85 nm) and at λ > 440 nm for the F-doped thick films. (t = 172 and 350 nm). The second, is the fluctuating region existing near the ultraviolet spectra for undoped and F-doped thin films (t = 85 nm). It is also clear from Fig. 5, that the values of n versus λ generally decrease with fluorine doping and increasing film thickness.

The value of n shows a considerable decrease for the film doped with 10% fluorine and having a thickness of 350 nm. X-ray diffraction results for this film (see Fig. 3) show higher crystallinity compared to other thin films. In addition, a large improvement in

TABLE II

No.	Material	Thickness, t (nm)	$\%T$ at 500 nm	R_s ($\Omega/\square$) at room temperature	$\phi(\times 10^{-3})$
1	Undoped SnO_2	85	0.97	509	1.45
2	SnO_2: F 10%	85	0.94	58	9.3
3	SnO_2: F 10%	172	0.90	20	17.4
4	SnO_2: F 10%	350	0.89	13	23.9

the grain size occurred for this film (Table I). It was also found that the fluctuating region observed for n–λ for other thin films prepared does not exist for this thicker F-doped film. The behaviour of the refractive index of our F-doped SnO_2 thick film is correlated with the extent of preferred orientation of microcrystallites along the (2 0 0) plane which increased rapidly for this thick F-doped film in comparison with other thin films (see Fig. 3). Thus, the high fluctuation in the refractive index near the ultraviolet region of our poorly crystalline undoped and doped thin films may result from the existence of multi-oriented SnO_2 microcrystallites, each orientation having a different refractive index. For the thick F-doped films, there is one main preferred orientation having a single value of refractive index. This result is in good agreement with that reported by Demiryont and Nietering [20] on SnO_2 prepared by two different techniques: thermal evaporation and spray pyrolysis.

The figure of merit, ϕ, is derived by Haacke [21] to predict the selective properties of transparent conductive coatings from the optical and electrical data and is given by

$$\phi = T^{10}/R_s \tag{11}$$

where T is the transmission and R_s is the sheet resistance. The results of optical transmission at solar maximum ($\simeq$ 500 nm), sheet resistance, and the figure of merit of undoped and F-doped SnO_2 films with different thickness are given in Table II.

It is clear from Table II that the values of sheet resistance, R_s, decrease sharply with fluorine doping. The figure of merit values of the undoped films increase seven times on doping with fluorine with the same film thickness; it also shows an increase with increasing film thickness. These highest values of figure of merit obtained are in agreement with those reported by other workers [22]. The abrupt decrease in sheet resistance at room temperature for F-doped films is associated with the increasing extent of crystallinity of the films, as found from X-ray diffraction results. The increased crystallinity reduces disorder and thereby increases the mobility [23]. It was also observed for F-doped films that the crystallite size increases (see Table I) and consequently scattering at grain boundaries decreases [6]. This will also lead to an increase in the mobility. On the other hand, when monovalent fluorine of ionic radius 0.136 nm acts as a dopant in tin oxide, it may substitute the divalent O anion of ionic radius 0.14 nm [24]. For every fluorine substitution in SnO_2, a tin atom retains an extra unpaired electron which enters the conduction band of the lattice and thereby the number of charge carriers increases. Thus the abrupt decrease in sheet resistance for F-doped film is attributed to an increase in both mobility and carrier concentration. This result is in good agreement with that reported by Bruneaux *et al.* [6].

To study the effect of fluorine doping on the energy gap of SnO_2, the direct energy gap was determined using the equation [25]

$$\alpha = \alpha_0(h\nu - E_0)^{1/2} \qquad h\nu > E_0 \tag{12}$$

$$\alpha = 0 \qquad h\nu < E_0 \tag{13}$$

where α is the absorption coefficient, $h\nu$ is the photon energy and E_0 is the energy band gap; α_0 is nearly constant and independent of photon energy. Calculations of the absorption coefficient, α, were carried out using the ratio of transmission of two films of different thickness, which is given by

$$T_{1-2} = e^{-\alpha\Delta t} \tag{14}$$

where T_{1-2} is the ratio of transmission and Δt is the difference in thickness of the two films. $\alpha\Delta t$ can then be accurately determined without knowing Δt. This was achieved in the present investigation by placing the thin sample in the reference beam and the thicker one in the sample beam of the recording spectrophotometer [26]. The direct band to band energy gap is determined by plotting $(\alpha\Delta t)^2$ as a function of photon energy $h\nu$ as shown in Figs 6 and 7. The energy gap is obtained by extrapolating the linear portion of the $(\alpha\Delta t)^2$–$h\nu$ plot to $(\alpha\Delta t)^2 = 0$. The value obtained for the direct energy gap is $\simeq$ 4.21 eV for fluorine-doped tin oxide films and $\simeq$ 4.11 eV for the undoped one. The energy gap value obtained for the low-resistance F-doped film is about 0.1 eV higher than that for the

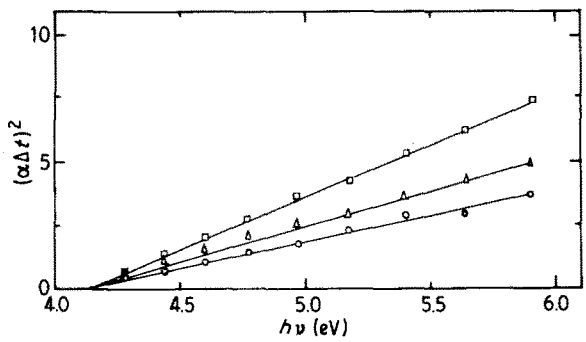

Figure 6 Variation of the square of the absorption coefficient as a function of the photon energy for different thicknesses of undoped SnO_2 thin films: t = (○) 25 nm, (△) 40 nm and (□) 85 nm.

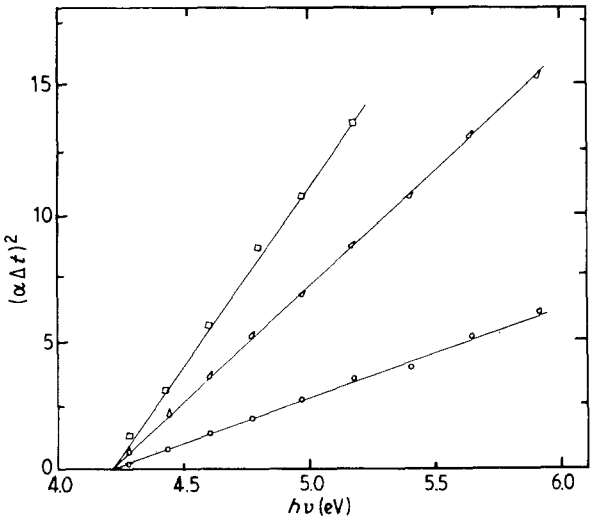

Figure 7 Variation of the square of the absorption coefficient as a function of the photon energy for different thicknesses of SnO_2: F doped thin films: t = (○) 85 nm, (△) 172 nm and (□) 350 nm.

high-resistance undoped film. Similar results are obtained by Shanthi *et al.* [3]. This phenomenon may be explained by assuming that the allowed states near the bottom of the conduction band are occupied to rather high levels and that the allowed transitions from the valence band would have correspondingly higher energies than the forbidden band gap. This band gap widening is also observed in In_2O_3 and In_2O_3: Sn and is interpreted on the basis of the effective mass model [27].

4. Conclusion

The large direct band gap of F-doped tin oxide films of 4.21 eV, high transparency in the visible region together with the low sheet resistance and refractive index (1.85) allow it to be used as an antireflection coating, as well as an electrode in solar cells. Moreover, the large value of the figure of merit reflects the suitability of the film for different applications in solar cells.

References

1. K.L. CHOPRA, S. MAJOR and D.K. PANDYA, *Thin solid films* **102** (1983) 1.
2. W. A. BADAWY, H. H. AFIFY and E. M. EIGIAR, *J. Electrochem. Soc.* **137** (1990) 1592.
3. E. SHANTHI, V. DUTTA, A. BANERJEE and K. L. CHOPRA, *J. Appl. Phys.* **51** (1980) 6243.
4. F. SIMONIS, M. VAN DER LEIJ and C. J. HOOGENDOOM, *Sol. Energy Mater.* **1** (1979) 221.
5. G. P. SKORNYAKOV and T. P. SURKOVA, *Sov. Phys. Semiconductor* **10** (1976) 1054.
6. J. BRUNEAUX, H. CACHET, M. FROMENT, M. LEVART and J. VEDEL, *J. Microsc. Spectrosc. Electron.* **14** (1989) 1.
7. W. C. HINDS, "Aerosol Technology" (Wiley, New York, 1982).
8. Inorganic index to Powder Diffraction File, ASTM, Powder Diffraction File, Card No. 5-0467 (American Society for Testing and Materials, Philadelphia, PA).
9. K. B. SUNDARAM and G. K. BHAGAVAT, *Thin Solid Films* **78** (1981) 35.
10. C. AGASHE, B. R. MARATHE, M. G. TAKAWALE and V. G. BHIDE, *ibid.* **164** (1988) 261.
11. M. U. COHEN, *Rev. Sci. Instrum.* **6** (1935) 68.
12. A. F. CARROLAND and L. H. SLACK, *J. Electrochem. Soc.* **123** (1976) 1889.
13. N. SRINIVASA MURTY and S. R. JAWALEKAR, *Thin Solid Films* **100** (1983) 219.
14. S. R. VISHWAKARMA, J. P. UPADHYAY and H. C. PRASAD, *ibid.* **176** (1989) 99.
15. B. CULLITY, "Elements of X-ray diffraction" (Addison-Wesley, London, 1955).
16. K. TOMINAGA, T. YUASA, M. KUME and O. TADA, *Jpn. J. Appl. Phys.* **24** (1985) 944.
17. H. CZTERNASTEK, A. BRUDNIK and M. JACHIMOWSKI, *Solid State Commun.* **65** (1988) 1025.
18. E. AKTULGA, PhD thesis, Department of Physics, Faculty of Science, Istanbul University, Istanbul, Turkey (1983).
19. H. DEMIRYONT, J. R. SITES and K. GEIB, *Appl. Opt.* **24** (1985) 490.
20. H. DEMIRYONT and K. E. NIETERING, *Sol. Energy Mater.* **19** (1989) 79.
21. G. HAACKE, *Appl. Phys. Lett.* **28** (1976) 622.
22. M. T. MOHAMMAD and W. A. ABDUL-GHAFOR, *Phys. Status Solidi (a)* **106** (1988) 479.
23. I. S. MULLA, H. S. SONI, V. RAO and A. P. B. SINHA, *J. Mater. Sci.* **21** (1986) 1280.
24. P. GROSSE and F. J. SCHMITTE, *Thin Solid Films* **90** (1982) 309.
25. A. K. ABASS, H. BAKR, S. A. JASSIM and T. A. FAHAD, *Sol. Energy Mater.* **17** (1988) 425.
26. O. P. AGNIHORRI, B. K. GUPTO and A. K. SHARMA, *J. Appl. Phys.* **49** (1978) 4540.
27. I. HAMBERG, C. G. GRANQVIST, K. F. BERGGREN, B. E. SERNELIVS and L. ENGSTROM, *Sol. Energy Mater.* **12** (1985) 479.

Received 30 July
and accepted 8 August 1990